Pergamon

J. Biomechanics, Vol. 29, No. 6, pp. 723–733, 1996

Printed in Great Britain
0021-9290/96 $15.00 + .00

0021-9290(95)00144-1

THE INFLUENCE OF MUSCLES ON KNEE FLEXION DURING THE SWING PHASE OF GAIT

Stephen J. Piazza* and Scott L. Delp†

*Department of Mechanical Engineering, Northwestern University and †Departments of Biomedical Engineering and Physical Medicine & Rehabilitation, Northwestern University, and Sensory Motor Performance Program, Rehabilitation Institute of Chicago, IL 60611, U.S.A.

Abstract—Although the movement of the leg during swing phase is often compared to the unforced motion of a compound pendulum, the muscles of the leg are active during swing and presumably influence its motion. To examine the roles of muscles in determining swing phase knee flexion, we developed a muscle-actuated forward-dynamic simulation of the swing phase of normal gait. Joint angles and angular velocities at toe-off were derived from experimental measurements, as were pelvis motions and muscle excitations. Joint angles and joint moments resulting from the simulation corresponded to experimental measurements made during normal gait. Muscular joint moments and initial joint angular velocities were altered to determine the effects of each upon peak knee flexion in swing phase. As expected, the simulation demonstrated that either increasing knee extension moment or decreasing toe-off knee flexion velocity decreased peak knee flexion. Decreasing hip flexion moment or increasing toe-off hip flexion velocity also caused substantial decreases in peak knee flexion. The rectus femoris muscle played an important role in regulating knee flexion; removal of the rectus femoris actuator from the model resulted in hyperflexion of the knee, whereas an increase in the excitation input to the rectus femoris actuator reduced knee flexion. These findings confirm that reduced knee flexion during the swing phase (stiff-knee gait) may be caused by overactivity of the rectus femoris. The simulations also suggest that weakened hip flexors and stance phase factors that determine the angular velocities of the knee and hip at toe-off may be responsible for decreased knee flexion during swing phase. Copyright © 1996 Elsevier Science Ltd.

Keywords: Gait; Swing phase; Knee flexion; Dynamic simulation; Rectus femoris.

INTRODUCTION

The beginning of swing phase is marked by flexion of the hip, knee, and ankle of the swing limb that draws the toe up and away from the ground as the limb moves forward. Knee flexion is especially important to toe clearance; without sufficient knee flexion in swing phase, the toe of the swing limb will strike the ground. Gage (1990) reported that knee flexion of approximately 60° is necessary to ensure toe clearance. Winter (1992) reported that mean toe clearance is only 1.29 cm in normal swing and that toe clearance is particularly sensitive to changes in knee angle.

The motion of the swing leg is often likened to the unforced swinging of a compound pendulum. The low level of activity in the leg muscles during swing (relative to stance) supports this characterization of swing phase as a 'ballistic' motion. In a simulation of swing phase, Mochon and McMahon (1980) found a range of initial segment angular velocities for which toe clearance was achieved without applied forces or moments representing the actions of muscles. Mena *et al.* (1981) also found that a near-normal swing could be simulated in the absence of moments applied to the thigh and shank segments. McGeer (1990) analyzed and built two-legged 'passive dynamic' machines with knees that are able to walk down slight slopes without forces or moments applied to represent the actions of muscles. Although these examples suggest that the swing leg is not muscle-driven, it is reasonable to expect that muscles do affect the motions of swing. The muscles of the leg exhibit stereotypical patterns of activity during swing and presumably generate forces that affect limb motion.

Knee flexion may be influenced by muscles that cross the knee and by muscular moments produced at other joints (via dynamic coupling). For example, Perry (1987) and Kerrigan *et al.* (1991) have theorized that a hip flexion moment not only flexes the hip but also flexes the knee in normal swing phase. Yamaguchi and Zajac (1990) found that hip flexion moment contributed to knee flexion through dynamic coupling in a computer simulation of human walking. In some pathologies, normal knee flexion seems to be prevented by the actions of muscles. For instance, patients with cerebral palsy who walk with decreased knee flexion in swing phase (termed stiff-knee gait) have difficulty achieving toe clearance without compensating by circumducting the hip or vaulting on the stance limb (Sutherland and Davis, 1993). Stiff-knee gait is frequently attributed to the knee-extending action of spastic quadriceps–especially the rectus femoris–during swing (Perry, 1987; Sutherland *et al.*,

Received in final form 5 *September* 1995.
Address correspondence to: Scott L. Delp, Ph.D., Sensory Motor Performance Program, Rehabilitation Institute of Chicago (Room 1406), 345 East Superior Street, Chicago, IL 60611, U.S.A.

1990; Damron *et al.*, 1993). However, the role of hip flexion moment (or its absence) in producing knee flexion during the swing phase of either normal of stiff-knee gait is presently unknown.

The ways in which *individual* muscles contribute to the motions of gait are not well known. Speculation about the function of a muscle during gait is often based only upon its activation pattern, anatomical position, and the concurrent motion of the spanned joint(s). However, previous studies have shown that it is also important to consider limb dynamics in analyses of muscle function (Hollerbach and Flash, 1982; Zajac and Gordon, 1989). Muscles have the potential to accelerate joints they do not cross and biarticular muscles may produce joint accelerations that oppose their joint moments; an analysis of muscle function that ignores limb dynamics does not allow for such possibilities. Information about individual muscles is difficult to obtain when muscle actions are modeled by moments applied to limb segments (Mena *et al.*, 1981) or about joints (Onyshko and Winter, 1980). However, an accurate dynamics simulation of swing phase in which muscle forces are applied to the skeleton may be used to interpret the functional roles of individual muscles.

We therefore developed a muscle-actuated, dynamic simulation of swing phase to test the following hypotheses: (1) muscles play a role in producing normal flexion of the knee joint in early swing phase; and (2) knee flexion in early swing phase may be inhibited by a decrease in muscular hip flexion moment. We specifically investigated the role of rectus femoris because overactivity of this muscle is thought to cause stiff-knee gait. Analysis of the rectus femoris is complex because it potentially increases knee flexion through its hip flexion moment and potentially decreases knee flexion through its knee extension moment.

METHODS

A model of the lower extremity and its muscles was developed to simulate swing phase dynamics. Experimentally derived muscle excitations and pelvis motions were input to the simulation, and computation of muscle forces and the motions of the swing limb were based upon these inputs. Details of the formulation of the model and of the swing phase simulation are given below.

Five segments were represented in the lower extremity model: the pelvis, thigh, patella, shank, and foot of the right leg (Fig. 1). Inertial properties for the thigh, shank, and foot segments (see Appendix) were specified using the regression equations of McConville *et al.* (1980) for a 180 cm, 75 kg male. The joints connecting the segments permitted motions in only the sagittal plane. The hip and ankle joints were modeled as frictionless revolutes, but the knee joint model included both the rolling and sliding of the femoral condyles on the tibial plateau and the patellofemoral kinematics (both of which depended only upon knee flexion angle), as described by Delp *et al.* (1990). Translation and tilt of the pelvis were prescribed throughout the simulation, leaving only three degrees of freedom: flexion–extension of the hip, knee, and ankle.

Forces representing muscle forces were applied to the segments throughout simulation of the swing phase. Each muscle (and its tendon) was modeled by an actuator that was characterized by four unique parameters: optimum fiber length l_o, maximum isometric force F_o, pennation angle, and tendon slack length (Zajac, 1989). The values used for these parameters and for the coordinates of muscle attachment sites on the segments were defined by Delp *et al.* (1990). All muscles were assumed to obey the same normalized force–velocity and force–length curves, and all muscles were assumed to have a maximum shortening velocity of $10 l_o\,s^{-1}$, as suggested by Zajac (1989) for muscles of mixed fiber type. The passive tension produced by each musculotendon actuator was determined by an exponential force–length curve which specified that passive tension was generated when the actuator's muscle fibers were stretched beyond l_o and that passive force equal to F_o was developed when fibers were stretched to $1.5 l_o$.

The input to each musculotendon actuator was a time-varying 'neural excitation' signal, $u(t)$, that determined muscle activation, $a(t)$, via first-order activation dynamics (Zajac, 1989):

$$\frac{da}{dt} = (u - a)(k_1 u + k_2), \tag{1}$$

where the activation and deactivation time constants were determined by

$$\tau_{act} = \frac{1}{k_1 + k_2} \tag{2}$$

and

$$\tau_{deact} = \frac{1}{k_2}. \tag{3}$$

The activation time constant, τ_{act}, was chosen to be 12 ms (Zajac, 1989) and the deactivation time constant, τ_{deact}, was chosen to be twice the value of the activation time constant, or 24 ms. The value of τ_{deact} was chosen arbitrarily, but the simulation was not sensitive to this choice; doubling or halving the value of τ_{deact} had very little effect on simulation output.

The formulation of a Hill-type model (Schutte, 1992) was used to represent musculotendon contraction dynamics. The equation governing contraction dynamics was of the form

$$\frac{dl_m}{dt} = f_v^{-1}(l_m, l_{mt}, a), \tag{4}$$

where l_m is muscle fiber length, l_{mt} is the total length of the musculotendon actuator, and f_v is the force–velocity relation. Thus, the time derivative of the fiber length (the fiber velocity) was found by first calculating the fiber force given the fiber length, musculotendon length, and activation, and then inverting the force–velocity curve.

Angle-dependent moments represented the effects of nonmuscular structures that cross the simulated hip and knee. Specifically, a hip flexion moment was applied

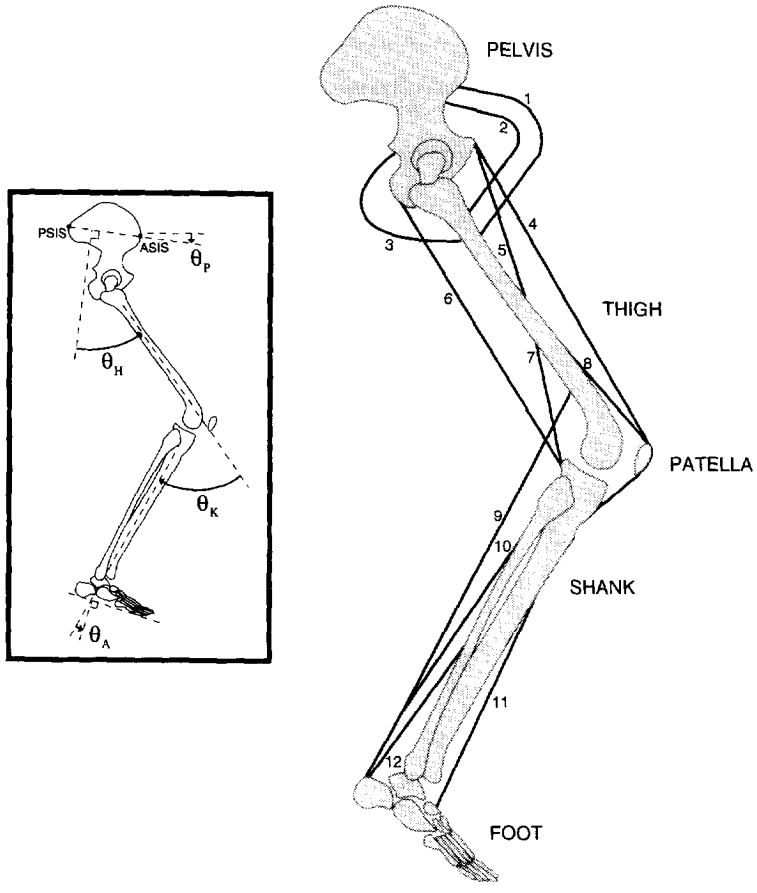

Fig. 1. Schematic drawing of the lower extremity model. All motions of the model were constrained to the sagittal plane. The model included 11 muscles: (1) iliacus, (2) psoas, (3) gluteus maximus, (4) rectus femoris, (5) adductor longus, (6) combined hamstrings muscles, (7) short head of biceps femoris, (8) combined vasti muscles, (9) gastrocnemius, (10) soleus, (11) pretibial group: combined tibialis anterior, extensor hallicus longus, and extensor digitorum longus, and (12) tibialis posterior. Muscle geometry is distorted for purposes of illustration. Inset: Hip angle was defined as the angle between the long axis of the thigh and the perpendicular of the line connecting the ASIS and PSIS. Knee angle was defined as the supplement of the angle formed by the long axes of the thigh and shank. Ankle angle was given by the angle formed by the long axis of the shank and the line perpendicular to the plantar surface of the foot. Anterior pelvic tilt, hip flexion, knee flexion, and ankle dorsiflexion each corresponded to a positive joint angle.

during initial swing when the hip was most extended, and a knee flexion moment was applied during late swing as the knee reached full extension. These moments were assumed to be exponential functions of joint angle:

$$\text{hip: } M_H^{NM}(\theta_H) = \begin{cases} 54.1\exp[-0.111(\theta_H + 9.96)], & \theta_H \leq 20^\circ, \\ 0 & \theta_H > 20^\circ, \end{cases} \quad (5)$$

$$\text{knee: } M_K^{NM}(\theta_K) = \begin{cases} 30.2\exp[-0.207(\theta_K - 0.030)], & \theta_K \leq 30^\circ, \\ 0 & \theta_K > 30^\circ, \end{cases} \quad (6)$$

where the nonmuscular hip and knee moments M_H^{NM} and M_K^{NM} are in N m, and the hip and knee angles, θ_H and θ_K, are in degrees. Audu and Davy (1985) proposed relationships representing the moments generated by uniarticular muscles and nonmuscular tissues that were derived by fitting double-exponential curves to measurements reported by Hatze (1976). Our hip and knee moment relations were derived by fitting single-exponential relations to the curves of Audu and Davy with the passive uniarticular muscle moments subtracted. However, we found that deriving M_H^{NM} in this fashion resulted in total (muscular and nonmuscular) hip flexion moments that were much larger than those measured during normal gait (Winter, 1991); for this reason we scaled M_H^{NM} to 75% of the value reported by Audu and Davy (1985).

We used the musculoskeletal model to simulate the swing phase (Fig. 2). The excitation inputs to the simulation were derived from the averaged intramuscular EMG (expressed as a percentage of maximum EMG) collected by Perry (1992) during normal gait. These experimental

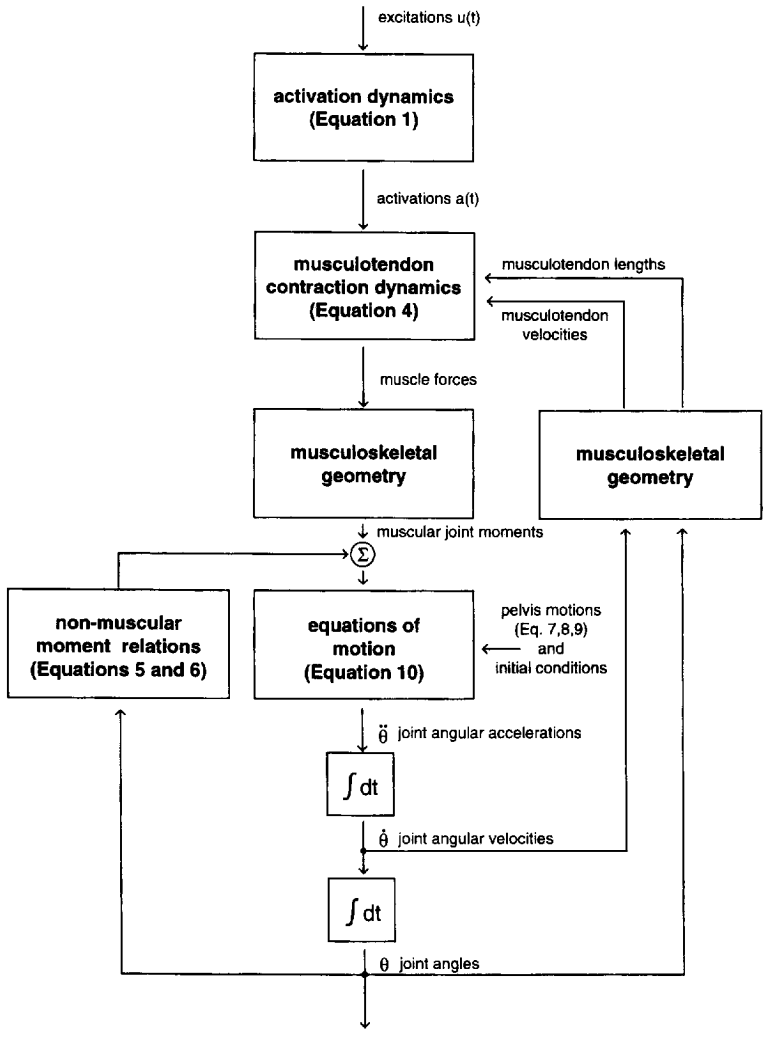

Fig. 2. Block diagram for the simulation of swing phase. Muscle activations were determined from muscle excitation inputs (approximated by EMG). The force generated by each musculotendon actuator was a function of its activation, length, and velocity. Total applied joint moments were calculated by multiplying muscular forces by moment arms and adding the angle-dependent non-muscular moments. The equations of motion were integrated in time to determine the kinematic output of the simulation. Hip joint center translation and pelvic tilt were prescribed from measured gait analysis data. Values for initial joint angles and angular velocities were also derived from experimental measurements.

EMG data were reported as functions of the gait cycle; to obtain excitations as functions of time, we assumed the duration of normal swing to be 0.42 s (Perry, 1992). The excitation signals used as input to the simulation were determined by approximating step functions to the experimental EMG measurements (Fig. 3); the use of step functions made it possible to vary the excitation inputs by varying at most three parameters (height, width, and time of onset).

Motions of the pelvis were prescribed throughout the simulation as functions of time based upon experimental data. We measured the gait kinematics of ten healthy subjects (age range = 6.9–24.7 yr; mean = 12.6 yr) using a Vicon (Oxford Metrics; Oxford, England) motion measurement system. A fifth-order polynomial was fit to the mean of the measured pelvic tilt angle and was used to prescribe pelvic tilt for the simulation. This function is given by

$$\theta_P(t) = 9.58 + 5.32t - 19.6t^2 + 358t^3 - 1290t^4 + 1210t^5 \quad (7)$$

where the units of $\theta_P(t)$ are degrees and t, the time elapsed after toe-off, is in seconds. The values prescribed for toe-off joint angles and angular velocities (Table 1) were also calculated from measurements of normal gait for this subject pool. The horizontal (x) and vertical (y) displacements of the pelvis were also prescribed as functions of time. These functions were derived by fitting linear and sine functions to averaged measurements of the hip center trajectory made for a group of six healthy adult subjects (age range = 18–31 yr; mean = 24 yr;

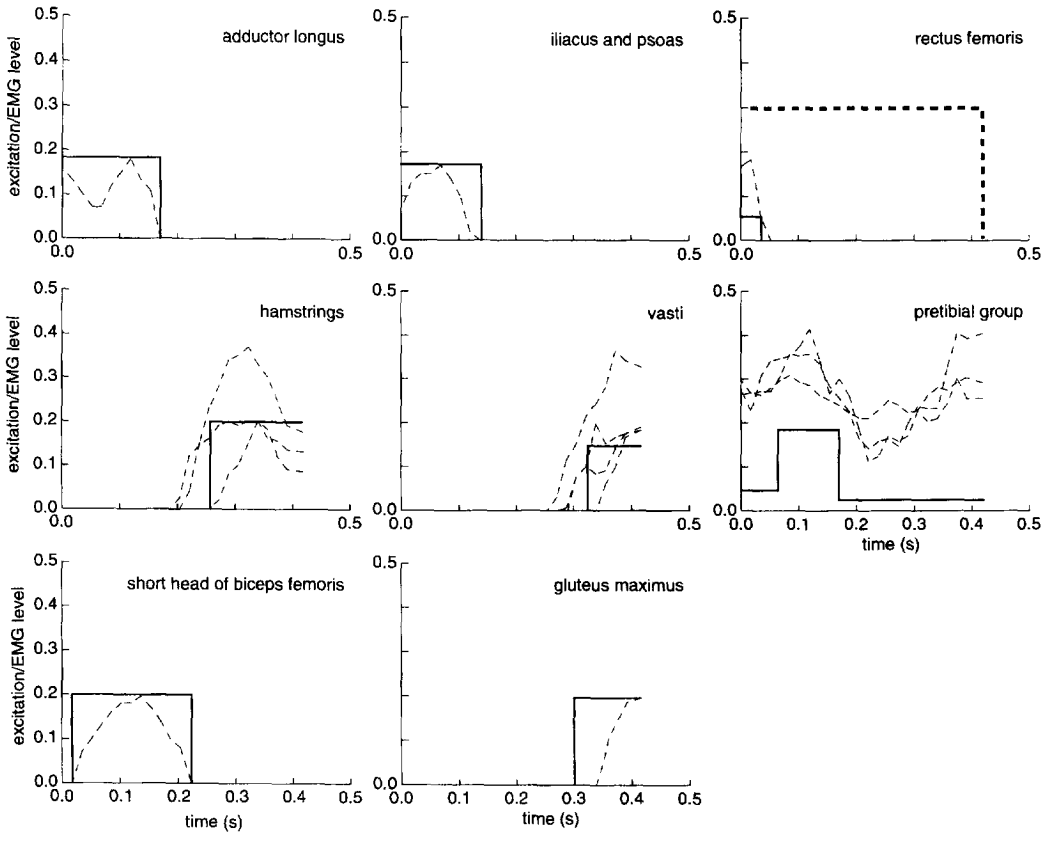

Fig. 3. Excitation signals, $u(t)$, input to the musculotendon actuators. Simulation inputs (solid lines) are step function approximations to the intramuscular EMG data (dashed lines) reported by Perry (1992). No excitation input was provided for soleus, gastrocnemius, or tibialis posterior. For actuators that represent combined muscles (hamstrings, vasti, and pretibial group), experimental EMG is shown for all of the constituent muscles. The iliacus and psoas actuators received the same excitation input. The thick dashed line shown for rectus femoris corresponds to the simulation performed with increased rectus femoris excitation.

Table 1. Measured joint angles and angular velocities at toe-off.

Parameter	Mean angle or angular velocity (deg or deg s^{-1})	Standard deviation (deg or deg s^{-1})
Hip flexion angle	− 1.2*	7.5
Knee flexion angle	39.5	10.2
Ankle dorsiflexion angle	− 8.8†	4.5
Hip flexion velocity	182	46
Knee flexion velocity	322	42
Ankle dorsiflexion velocity	− 109†	106

*Negative hip angle indicates extension.
†Negative ankle angle indicates plantarflexion; negative ankle dorsiflexion velocity indicates that the ankle is plantarflexing at toe-off.

height range = 172–185 cm; mean = 179 cm), and are given by

$$x(t) = 1.17t, \tag{8}$$

$$y(t) = 0.026\sin(8.4t - 0.080), \tag{9}$$

where $x(t)$ and $y(t)$ are expressed in meters.

The simulation was implemented on a Silicon Graphics (Mountain View, CA) workstation using two dynamic simulation software packages: Dynamics Pipeline (MusculoGraphics, Inc.; Evanston, IL) and SD/FAST (Symbolic Dynamics, Inc.; Mountain View, CA). The equations of motion for the model were integrated forward in time using SD/FAST, which employs a variable time step method based on a fourth-order Runge–Kutta–Merson step.

We performed a 'one-at-a-time' factorial analysis (Hogg and Ledolter, 1987) to determine the capability of each of the joint moments and initial angular velocities to diminish peak knee flexion in swing. Each joint angular velocity was varied from its normal swing simulation value by two standard deviations (Table 1). Muscular joint moments equal to twice the joint moment standard deviation were added to or subtracted from the normal simulation joint moment at each time step during the simulation. The standard deviations of the muscular joint moments were approximated by averaging the standard deviations calculated by Winter (1991) over the duration of the swing phase. The change in peak knee flexion and the change in minimum toe height that resulted from each altered joint moment and initial angular velocity were determined.

A simulation of swing phase was performed with the rectus femoris actuator removed from the model, and another simulation was performed with a prolonged and exaggerated excitation input to the rectus femoris actuator. The purpose of these simulations was to clarify the role of the rectus femoris in producing normal knee flexion. For the latter simulation, the excitation input to the rectus femoris actuator continued throughout the swing phase at 30% of its maximum level (as opposed to 0.03 s and 5% for the normal simulation; see Fig. 3).

The equations of motion of the swing leg system were used to assess which factors contribute to angular acceleration at the knee. A Lagrangian formulation was used to derive the equations of motion after a frictionless revolute was substituted for the knee joint. The equations were expressed in matrix form:

$$\mathbf{M}\begin{bmatrix} \ddot{\theta}_H \\ -\ddot{\theta}_K \\ \ddot{\theta}_A \end{bmatrix} = \mathbf{C}\begin{bmatrix} \dot{\theta}_H^2 \\ \dot{\theta}_K^2 \\ \dot{\theta}_A^2 \end{bmatrix} + \mathbf{V}\begin{bmatrix} -\dot{\theta}_H\dot{\theta}_K \\ \dot{\theta}_H\dot{\theta}_A \\ -\dot{\theta}_K\dot{\theta}_A \end{bmatrix} + \mathbf{P}\begin{bmatrix} \ddot{x} \\ \ddot{y} \end{bmatrix} + \mathbf{G} + \begin{bmatrix} M_H \\ -M_K \\ M_A \end{bmatrix}, \quad (10)$$

where θ_H, θ_K, and θ_A are the joint angles; M_H, M_K, and M_A are the joint moments applied to the model by musculotendon actuators and non-muscular joint springs; x and y are the horizontal and vertical displacements of the pelvis relative to a ground-fixed reference frame; and the matrices **M**, **C**, **V**, **P**, and **G** depend upon joint angles and inertial parameters (see the appendix for a full account of the components of these matrices).

The mass matrix **M** was found to be full rank and thus invertible throughout the simulation. Premultiplying both sides of equation (10) by $\mathbf{M}^{-1}$ gives

$$\begin{bmatrix} \ddot{\theta}_H \\ -\ddot{\theta}_K \\ \ddot{\theta}_A \end{bmatrix} = \mathbf{M}^{-1}\mathbf{C}\begin{bmatrix} \dot{\theta}_H^2 \\ \dot{\theta}_K^2 \\ \dot{\theta}_A^2 \end{bmatrix} + \mathbf{M}^{-1}\mathbf{V}\begin{bmatrix} -\dot{\theta}_H\dot{\theta}_K \\ \dot{\theta}_H\dot{\theta}_A \\ -\dot{\theta}_K\dot{\theta}_A \end{bmatrix} + \mathbf{M}^{-1}\mathbf{P}\begin{bmatrix} \ddot{x} \\ \ddot{y} \end{bmatrix} + \mathbf{M}^{-1}\mathbf{G} + \mathbf{M}^{-1}\begin{bmatrix} M_H \\ -M_K \\ M_A \end{bmatrix}. \quad (11)$$

Using equation (11), the joint angular accelerations of the hip, knee, and ankle were separated into four component accelerations that were caused by (1) combined Coriolis and centrifugal effects, (2) pelvis translation, (3) gravity, and (4) muscles. Each term on the right-hand side of equation (11) was calculated at each time step using the kinematic output (joint angles and joint angular velocities) and the history of muscle-applied moments for the simulation of normal swing phase. The muscle-related acceleration term [on the far right in equation (11)] was divided first into joint angular accelerations caused by each muscular joint moment and further into joint angular accelerations caused by individual muscles.

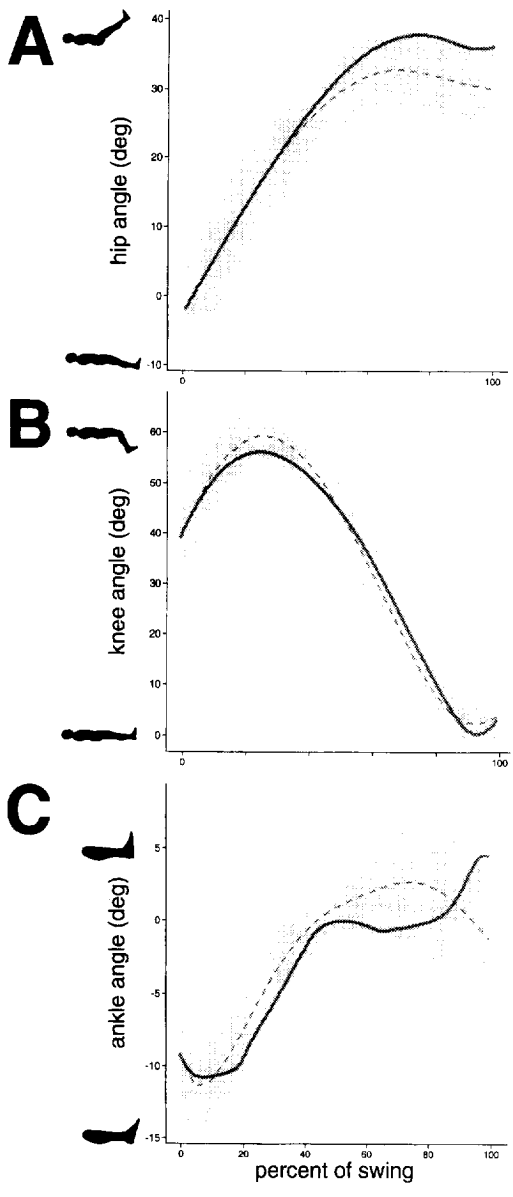

Fig. 4. Hip (A), knee (B), and ankle (C) angles versus percent of swing. Solid curves represent simulation output; dashed curves with shading represent measured mean joint angles plus and minus one standard deviation for normal swing.

RESULTS

The joint angle trajectories produced by the simulation approximated our experimental measurements made for normal gait (Fig. 4). The simulated knee flexed to 57° following toe-off and the simulated toe cleared the ground. In late swing, however, our simulation exhibited an excess of ankle dorsiflexion.

Factorial analysis revealed that a large decrease in hip flexion moment produced a substantial reduction in peak knee flexion (Fig. 5). Increasing knee extension moment and decreasing initial knee angular velocity each had the expected effect of decreasing peak knee flexion. An increase in hip flexion velocity at toe-off also decreased

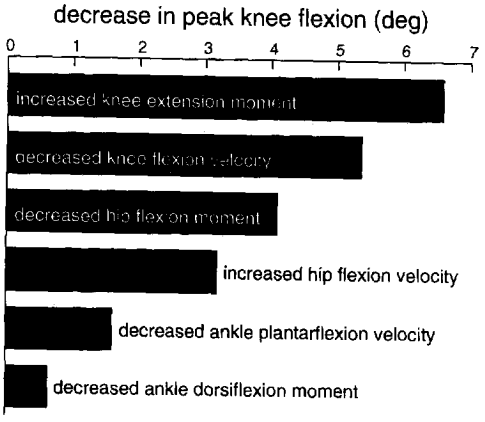

Fig. 5. Decrease in peak knee flexion corresponding to a two-standard-deviation change in each muscular joint moment and toe-off joint angular velocity.

knee flexion in swing phase. Specifically, a two-standard-deviation change (in the direction indicated in Fig. 5) in the knee extension moment, initial knee flexion velocity, hip flexion moment, and initial hip flexion velocity decreased peak knee flexion by 6.6, 5.4, 4.1, and 3.2°, respectively. These changes were considered important because they were accompanied by decreases in minimum toe height of 2.92, 1.29, 1.33, and 1.72 cm, respectively; all of which are at least as large as the 1.29 cm average minimum toe clearance reported by Winter (1992) for normal gait. Changes in initial ankle velocity and ankle moment also affected peak knee flexion, but to a lesser extent.

Rectus femoris was found to play an important role in regulating knee flexion during swing phase. A simulation of swing performed with the rectus femoris actuator removed resulted in excessive knee flexion, suggesting that the knee-extending action of the rectus femoris in early swing is important for normal knee flexion (Fig. 6). Conversely, overactivity in rectus femoris inhibited knee flexion in the simulation; an increase in the excitation input to the rectus femoris actuator caused a decrease in knee flexion.

In early swing the muscles acted to brake the rapid toe-off knee flexion velocity; the net muscle-induced acceleration of the knee during this period was in the extension direction. The rectus femoris actuator produced a knee extension acceleration prior to peak knee flexion, as did the passive vasti actuator (though the vasti-induced acceleration was only 50% of the acceleration induced by rectus femoris on average). Knee flexion acceleration in early swing was produced by the actuators representing hip flexors, the biceps femoris (short head), the pretibial group, and the nonmuscular hip flexion moment [equation (5)]. Gravitational, coriolis, and centrifugal forces collectively caused a knee extension acceleration throughout the swing.

We unexpectedly found that the gastrocnemius muscle produced a knee *extension* acceleration between 25 and 60% of swing while simultaneously producing a knee

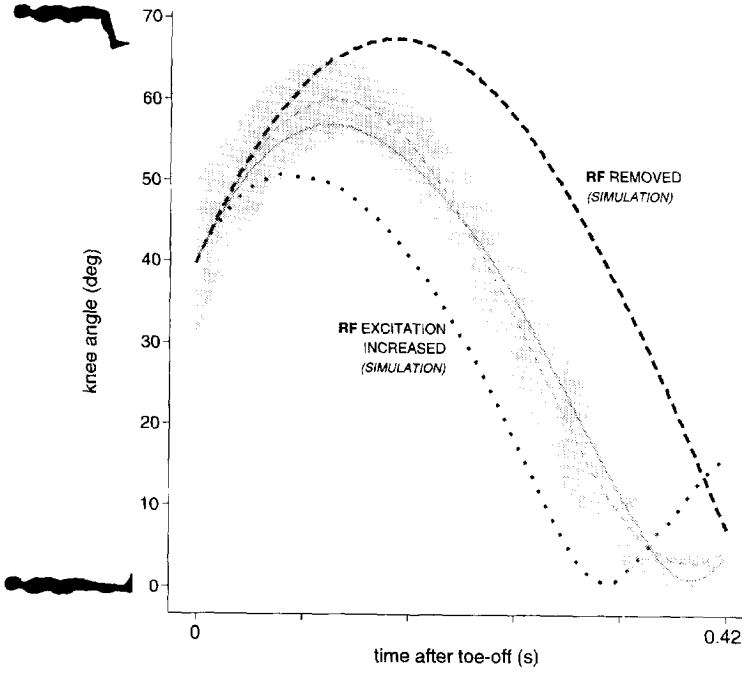

Fig. 6. Knee angle versus time for simulations performed with the rectus femoris (RF) actuator removed and with increased and extended excitation of the rectus femoris. The dashed curve with shading represents measured mean joint angle plus and minus one standard deviation for normal swing. The solid curve within the shaded area represents the knee angle for a simulation performed with all musculotendon actuators intact and supplied with normal excitations. Removal of the rectus femoris both prolonged and exaggerated knee flexion; increased rectus femoris activity decreased knee flexion.

flexion moment. Though the gastrocnemius was not active, it generated force during the simulation when it was passively stretched. Other biarticular actuators produced accelerations opposite in direction to their joint moments: the hamstrings produced a hip flexion acceleration in mid-swing and rectus femoris produced a hip extension acceleration in early swing.

DISCUSSION

In this study, a muscle-actuated, dynamic simulation was developed to analyze how muscle actions affect flexion of the knee during the early part of the swing phase of normal gait. We found that normal knee flexion is determined by a large knee flexion velocity at toe-off which is tempered by the knee-extending action of the rectus femoris and vasti muscles. Lack of muscular hip flexion moment was found to inhibit knee flexion in early swing.

The inputs and outputs of our simulation approximated data reported in the literature. The initial joint angles used in the simulation were similar to those reported by Kadaba *et al.* (1990) at 62% of the gait cycle. Simulation joint angles (Fig. 4) compare favorably to data reported by Kadaba *et al.* (1990) and Perry (1992). We judged excessive ankle dorsiflexion and hip flexion in late swing to be tolerable because we were more concerned with accurately modeling early swing (the time of peak knee flexion). The sum of joint moments produced by muscles and nonmuscular joint springs in the simulation were similar to the swing phase joint moments reported by Winter (1991), who used an inverse-dynamic formulation to calculate muscular joint moments from measured joint angular kinematics (Fig. 7).

We tried to base our simulation on experimentally derived data wherever possible. Unfortunately, practical considerations dictated that we could not obtain all the experimental data we needed from a single source. We drew simulation parameters and input data from several sources in the literature as well as from our own measurements. Initial conditions for the simulation were determined using data collected from a subject pool that included children over age seven; we believe that the inclusion of children's data was justified by the finding of Sutherland *et al.* (1980) that an adult gait pattern is attained by age seven. However, it was necessary to measure pelvis translation in a different pool of adult subjects because we expected these data to be smaller in children.

By modeling the motions of only the swing leg, we have neglected to model explicitly the motions and muscular forces produced in other parts of the body. Mochon and McMahon (1980) found that inclusion of the stance limb was necessary to achieve times of swing that approximated experimental measurements. However, the influences of such factors upon the motions of the swing leg were presumably accounted for in the present model by the prescribed pelvis translation [the third term from the right in equation (11)].

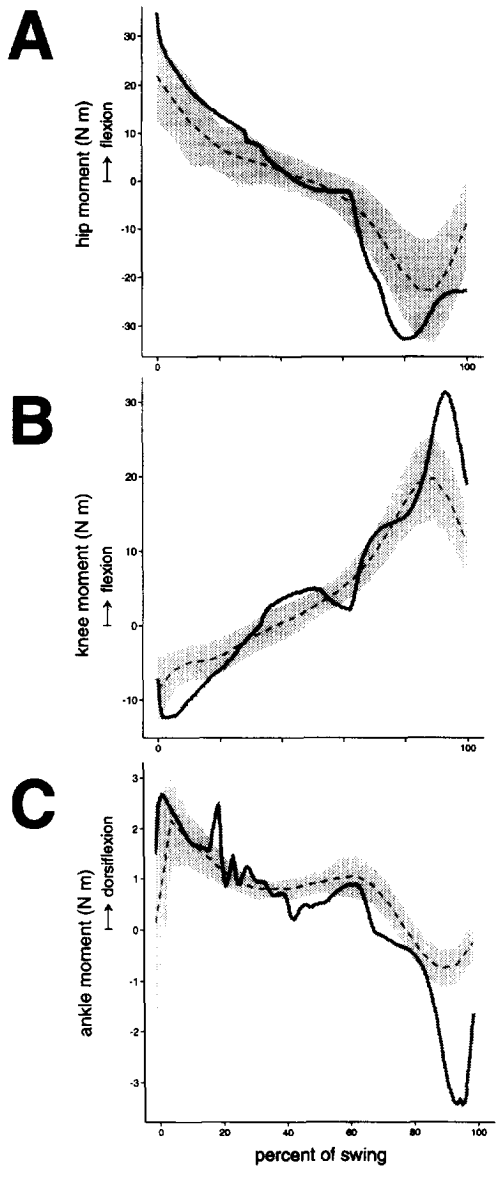

Fig. 7. Muscular hip (A), knee (B), and ankle (C) moments versus percent of swing. Solid curves represent simulation output; dashed curves with shading represent mean muscular joint moments plus and minus one standard deviation as calculated by Winter (1991) for the normal swing, based on an inverse-dynamic formulation. The abrupt changes in the hip and knee moments at approximately 65% of swing are caused by the hamstrings actuator becoming active at that time.

The one-at-a-time factorial analysis that was employed neglects the effects of combined variation among the factors. A more elaborate analysis would entail the covariation of all three initial joint angular velocities and all three joint moments. Such an analysis would require that 729 (3^6) simulations be run, as opposed to 13 ($2 \cdot 6 + 1$) simulations for the one-at-a-time approach. However, a full factorial analysis would be helpful for understanding how factors combine to affect peak knee flexion.

Our conclusion that the actions of muscles are necessary to check the large knee flexion velocity normally

Table 2. Comparison of knee flexion velocities at toe-off.

Source	Initial knee flexion velocity (deg s^{-1})
Mena *et al.* (1981)	237
Kadaba *et al.* (1990)	327
Present study	322
Mochon and McMahon (1980)*	166–286

*Approximate range for which Mochon and McMahon (1980) reported that 'ballistic' swing is possible.

present in early swing (Fig. 7) is consistent with the findings of those who have analyzed above-knee prosthetic gait. Menkveld *et al.* (1981) and Hicks *et al.* (1985) found that the knee extension moment generated by a damped knee component is necessary to prevent excessive knee flexion. This conclusion contradicts the findings of Mena *et al.* (1981), who suggested that normal swing phase could be simulated in the absence of muscular knee moment. A comparison of toe-off knee flexion velocities (Table 2) explains this apparent contradiction. The initial knee flexion velocity used by Mena *et al.* (1981) is substantially smaller than either the slope at 62% of the gait cycle of the averaged knee angle versus time curve reported by Kadaba *et al.* (1990) or the mean toe-off velocity measured in the present study (237° s^{-1} versus 327 or 322° s^{-1}). Mochon and McMahon (1980) found that swing could occur without muscular moments only over a range of initial knee flexion velocities that excludes both of the values measured for normal gait; this further supports the conclusion that muscular action is necessary to affect a normal knee flexion pattern in most normal subjects. It is possible that the use of muscles to restrain knee flexion in early swing is not needed if toe-off knee flexion velocity is reduced, as occurs in slow walking. Murray *et al.* (1984) found that both rectus femoris activity and toe-off knee flexion velocity (estimated from the slope of the reported mean knee angle trajectory) decreased with walking speed, though peak knee flexion in swing did not. Patients who walk with stiff-knee gait have been found to walk at low speeds (Kerrigan *et al.*, 1991) but are, perhaps, unable to duplicate the reduction in toe-off rectus fermoris activity that appears in the slow gait of unimpaired subjects.

Those who have attempted to identify the biomechanical determinants of stiff-knee gait have often cited only spasticity of the quadriceps during swing as the cause (Sutherland *et al.*, 1990; Damron *et al.*, 1993). We agree that the lack of swing phase knee flexion associated with stiff-knee gait might be caused by an increased knee extension moment that would accompany overactive quadriceps. The results of the present study, however, suggest that altered knee and hip flexion velocities at toe-off and decreased hip flexion moment may also contribute to decreased knee flexion (Fig. 5). Thus, the determinants of the toe-off knee and hip angular velocities and weakened hip flexors are also possible causes of stiff-knee gait.

Our finding that the gastrocnemius acts to extend the knee in swing was unexpected because the gastrocnemius passes posterior to the knee. Knee extension acceleration by a muscle that produces a knee flexion moment is made possible by the coupled nature of the system dynamics (Zajac and Gordon, 1989). Gastrocnemius is a biarticular muscle that produces a knee flexion moment and an ankle plantarflexion moment. These moments produce opposing accelerations of the knee joint: knee flexion moment accelerates the knee in flexion and ankle plantarflexion moment accelerates the knee in extension. If the latter acceleration is larger than the former, a net knee extension acceleration results. The direction of the gastrocnemius-induced acceleration at the knee is determined by the muscle moment arm at each joint and the components of the inverse of the inertia matrix [$\mathbf{M}^{-1}$ in equation (11)], which transforms joint moments into joint angular accelerations.

The actions of an individual muscle are often inferred from EMG recordings and from the moments generated by the muscle. We have concluded from the results of our muscle-actuated simulations that an accurate assessment of the function of a muscle at a particular time during gait must account for the force-generating properties of the muscle, the musculoskeletal geometry, and the coupled nature of the system dynamics. Although we have focused on normal gait in this study, characterizing the accelerations caused by muscles during walking may also be helpful for understanding which muscles contribute to abnormal gait and for planning surgical procedures that alter the actions of muscles to correct pathological gait.

Acknowledgements—We are grateful to Carolyn Moore, Claudia Kelp-Lenane, Tony Weyers, and Steve Vankoski of the Gait Analysis Laboratory at Children's Memorial Hospital in Chicago for providing us with gait data. We would also like to thank Abraham Komattu and Peter Loan for assistance with the computer implementation of the simulation, Lisa Schutte for discussions regarding the formulation of the muscle model, and MusculoGraphics, Inc. for its donation of musculoskeletal modeling software. This work was supported by NSF Grant BCS-9257229.

REFERENCES

Audu, M. L. and Davy, D. T. (1985) The influence of muscle model complexity in musculoskeletal motion modeling. *J. Biomech. Engng.* **107,** 147–157.

Damron, T. A., Breed, A. L. and Cook, T. (1993) Diminished knee flexion after hamstring surgery in cerebral palsy: prevalence and severity. *J. Pediatric Orthop.* **13,** 188–191.

Delp, S. L., Loan, J. P., Hoy, M. G. Zajac, F. E., Topp, E. L. and Rosen, J. M. (1990) An interactive graphics-based model of the lower extremity to study orthopaedic surgical procedures. *IEEE Trans. Biomed. Engng.* **37,** 757–767.

Gage, J. R. (1990) Surgical treatment of knee dysfunction in cerebral palsy. *Clin. Orthop. Rel. Res.* **253,** 45–54.

Hatze, H. (1976) The complete optimization of a human motion. *Math. Biosci.* **28,** 99–135.

Hicks, R., Tashman, S., Altman, R. F. and Gage, J. R. (1985) Swing phase control with knee friction in juvenile amputees, *J. Orthop. Res.* **3,** 198–201.

Hogg, R. V. and Ledolter, J. (1987), *Engineering Statistics*. Macmillan, New York.
Hollerbach, J. M. and Flash, T. (1982) Dynamic interactions between limb segments during planar arm movement. *Biol. Cybernet.* **44**, 67–77.
Kadaba, M. P., Ramakrishnan, H. K. and Wootten, M. E. (1990) Measurement of lower extremity kinematics during level walking. *J. Orthop. Res.* **8**, 383–392.
Kerrigan, D. C., Gronley, J. and Perry, J. (1991) Stiff-legged gait in spastic paresis. *Am. J. Phys. Med. Rehabil.* **70**, 294–300.
McConville, J. T., Churchill, T. D., Kaleps, I., Clauser, C. E. and Cuzzi, J. (1980) Anthropometric relationships of body and body segment moments of inertia. Technical Report AFAMRL-TR-80-119, Air Force Aerospace Medical Research Laboratory, Wright-Patterson Air Force Base, OH.
McGeer, T. (1990) Passive dynamic walking. *Int. J. Robotics Res.* **9**, 62–82.
Mena, D., Mansour, J. M. and Simon, S. R. (1981) Analysis and synthesis of human swing leg motion duing gait and its clinical applications. *J. Biomechanics* **14**, 823–832.
Menkveld, S., Mansour, J. M. and Simon, S. R. (1981) Mass distribution in prosthetics and orthotics: quantitative analysis of gait using a biomechanical model simulation. Transactions of the 27th Annual Meeting of the Orthopaedic Research Society, p. 228.
Mochon, S. and McMahon, T. A. (1980) Ballistic walking. *J. Biomechanics* **13**, 49–57.
Murray, M. P., Mollinger, L. A., Gardner, G. M. and Sepic, S. B. (1984) Kinematic and EMG patterns during slow, free, and fast walking. *J. Orthop. Res.* **2**, 272–280.
Onyshko, S. and Winter, D. A. (1980) A mathematical model for the dynamics of human locomotion. *J. Biomechanics* **13**, 361–368.
Perry, J. (1987) Distal rectus femoris transfer. *Dew. Med. Child Neurol.* **29**, 153–158.
Perry, J. (1992) *Gait Analysis*. SLACK, Thorofare, NJ.
Schutte, L. M. (1992) Using musculoskeletal models to explore strategies for improving performance in electrical stimulation-induced leg cycle ergometry, Stanford University, Ph. D. thesis.
Sutherland, D. H. and Davids, J. R. (1993) Common gait abnormalities of the knee in cerebral palsy. *Clin. Orthop. Rel. Res.* **288**, 139–147.
Sutherland, D. H., Olshen, R., Cooper, L. and Woo, S. L.-Y. (1980) The development of mature gait. *J. Bone Jt Surg.* **62A**, 336–353.
Sutherland, D. H., Santi, M. and Abel, M. F. (1990) Treatment of stiff-knee gait in cerebral palsy: a comparison by gait analysis of distal rectus femoris transfer versus proximal rectus release. *J. Pediatric Orthop.* **10**, 433–441.
Winter, D. A. (1991) *Biomechanics of Motor Control and Human Gait*. University of Waterloo Press, Waterloo, Ontario, Canada.
Winter, D. A. (1992) Foot trajectory in human gait: a precise and multifactorial motor control task. *Phys. Ther.* **72**, 45–56.
Yamaguchi, G. T. and Zajac, F. E. (1990) Restoring unassisted natural gait to paraplegics via functional neuromuscular stimulation: a computer simulation study. *IEEE Trans. Biomed. Engng.* **37**, 886–902.
Zajac, F. E. (1989) Muscle and tendon: properties, models, scaling, and application to biomechanics and motor control. *Crit. Rev. Biomed. Engng.* **17**, 359–411.
Zajac, F. E. and Gordon, M. E. (1989) Determining muscle's force and action in multi-articular movement. *Exerc. Sport Sci. Rev.* **17**, 187–230.

APPENDIX

The components of the coefficient matrices in the matrix equation of motion [Equation (10)] are

$$\mathbf{M}_{11} = C_1 + 2C_6\cos\hat{\theta}_K + 2C_8\cos(\hat{\theta}_K + \hat{\theta}_A) + 2C_9\cos\hat{\theta}_A,$$

$$\mathbf{M}_{21} = C_2 + C_6\cos\hat{\theta}_K + C_8\cos(\hat{\theta}_K + \hat{\theta}_A) + 2C_9\cos\hat{\theta}_A,$$

$$\mathbf{M}_{31} = C_3 + C_8\cos(\hat{\theta}_K + \hat{\theta}_A) + C_9\cos\hat{\theta}_A,$$

$$\mathbf{M}_{12} = C_2 + C_6\cos\hat{\theta}_K + C_8\cos(\hat{\theta}_K + \hat{\theta}_A) + 2C_9\cos\hat{\theta}_A,$$

$$M_{22} = C_2 + 2C_9\cos\hat{\theta}_A,$$

$$M_{32} = C_3 + C_9\cos\hat{\theta}_A,$$

$$\mathbf{M}_{13} = C_3 + C_8\cos(\hat{\theta}_K + \hat{\theta}_A) + C_9\cos\hat{\theta}_A,$$

$$\mathbf{M}_{23} = C_3 + C_9\cos\hat{\theta}_A,$$

$$\mathbf{M}_{33} = C_3.$$

$$\mathbf{C}_{11} = 0,$$

$$\mathbf{C}_{21} = -C_6\sin\hat{\theta}_K - C_8\sin(\hat{\theta}_K + \hat{\theta}_A),$$

$$\mathbf{C}_{31} = -C_8\sin(\hat{\theta}_K + \hat{\theta}_A) - C_9\sin\hat{\theta}_A,$$

$$\mathbf{C}_{12} = C_6\sin\hat{\theta}_K + C_8\sin(\hat{\theta}_K + \hat{\theta}_A),$$

$$\mathbf{C}_{22} = 0,$$

$$\mathbf{C}_{32} = -C_9\sin\hat{\theta}_A,$$

$$\mathbf{C}_{13} = C_8\sin(\hat{\theta}_K + \hat{\theta}_A) + C_9\sin\hat{\theta}_A,$$

$$\mathbf{C}_{23} = C_9\sin\hat{\theta}_A$$

$$\mathbf{C}_{33} = 0.$$

$$\mathbf{V}_{11} = 2C_6\sin\hat{\theta}_K + 2C_8\sin(\hat{\theta}_K + \hat{\theta}_A),$$

$$\mathbf{V}_{21} = 0,$$

$$\mathbf{V}_{31} = -2C_9\sin\hat{\theta}_A,$$

$$\mathbf{V}_{12} = 2C_8\sin(\hat{\theta}_K + \hat{\theta}_A) + 2C_9\sin\hat{\theta}_A,$$

$$\mathbf{V}_{22} = 2C_9\sin\hat{\theta}_A,$$

$$\mathbf{V}_{32} = 0,$$

$$\mathbf{V}_{13} = 2C_8\sin(\hat{\theta}_K + \hat{\theta}_A) + 2C_9\sin\hat{\theta}_A,$$

$$\mathbf{V}_{23} = 2C_9\sin\hat{\theta}_A,$$

$$\mathbf{V}_{33} = 0.$$

$$\mathbf{P}_{11} = C_4\cos\theta_H - C_5\cos(\theta_H + \hat{\theta}_K) - C_7\cos(\theta_H + \hat{\theta}_K + \hat{\theta}_A),$$

$$\mathbf{P}_{21} = -C_5\cos(\theta_H + \hat{\theta}_K) - C_7\cos(\theta_H + \hat{\theta}_K + \hat{\theta}_A),$$

$$\mathbf{P}_{31} = -C_7\cos(\theta_H + \hat{\theta}_K + \hat{\theta}_A),$$

$$\mathbf{P}_{12} = -C_4\sin\theta_H - C_5\sin(\theta_H + \hat{\theta}_K) - C_7\sin(\theta_H + \hat{\theta}_K + \hat{\theta}_A),$$

$$\mathbf{P}_{22} = -C_5\sin(\theta_H + \hat{\theta}_K) - C_7\sin(\theta_H + \hat{\theta}_K + \hat{\theta}_A),$$

$$\mathbf{P}_{32} = -C_7\sin(\theta_H + \hat{\theta}_K + \hat{\theta}_A).$$

$$\mathbf{G}_1 = -C_{10}\sin\theta_H - C_{11}\sin(\theta_H + \hat{\theta}_K) - C_{12}\sin(\theta_H + \hat{\theta}_K + \hat{\theta}_A),$$

$$\mathbf{G}_2 = -C_{11}\sin(\theta_H + \hat{\theta}_K) - C_{12}\sin(\theta_H + \hat{\theta}_K + \hat{\theta}_A),$$

$$\mathbf{G}_3 = -C_{12}\sin(\theta_H + \hat{\theta}_K + \hat{\theta}_A).$$

The constants C_1–C_{12} depend on the inertial parameters of the segments and are given by

$$C_1 = m_T d_T^2 + m_S(l_T^2 + d_S^2) + m_F(l_T^2 + l_S^2 + d_F^2) + I_T + I_S + I_F,$$

$$C_2 = m_S d_S^2 + m_F(l_S^2 + d_F^2) + I_S + I_F,$$

$$C_3 = m_F d_F^2 + I_F,$$

$$C_4 = m_T d_T + m_S l_T + m_F l_T,$$

$$C_5 = m_S d_S + m_F l_S,$$

$$C_6 = m_S l_T d_S + m_F l_T l_S,$$

$$C_7 = m_F d_F,$$

$$C_8 = m_F l_T d_F,$$

$$C_9 = m_F l_S d_F,$$

$$C_{10} = (m_T d_T + m_S l_T + m_F l_T) g,$$

$$C_{11} = (m_S d_S + m_F l_S) g,$$

$$C_{12} = m_F d_F g.$$

The hip flexion angle is represented by θ_H. The adjusted knee and ankle flexion angles are defined by: $\hat{\theta}_K = -\theta_K$ and $\hat{\theta}_A = \theta_A + 36.5°$; adjustments to θ_K and θ_A (which were defined to reflect commonly used clinical measures) were performed to write the equations more concisely.

The acceleration due to gravity is given by g and the inertial parameters of the segments are given in Table A1.

Table A1. Segment inertial parameters

Parameter	Symbol	Value
Masses	m_T	9.74 kg
	m_S	3.86 kg
	m_F	0.99 kg
Moments of inertia (I_{zz})	I_T	0.167 kg m^2
	I_S	0.060 kg m^2
	I_F	0.005 kg m^2
Lengths	l_T	0.40 m
	l_S	0.43 m
Distances from proximal end to center of mass	d_T	0.20 m
	d_S	0.15 m
	d_F	0.08 m

Because all pelvis motions were prescribed, the values assigned for the pelvis inertial parameters did not influence the simulation. Mass and moment of inertia were estimated for the patella (0.025 kg and 0.005 kg m^2, respectively). The simulation was not sensitive to these values; kinematic output was similar when these estimates were either increased or decreased fivefold.